



Published in final edited form as:

Behav Brain Res. 2017 June 30; 329: 111–119. doi:10.1016/j.bbr.2017.04.041.

Vulnerability of white matter tracts and cognition to the *SOD2* polymorphism: A preliminary study of antioxidant defense genes in brain aging

Lauren E. Salminen^{a,1}, Peter R. Schofield^{b,c}, Kerrie D. Pierce^c, Steven E. Bruce^a, Michael G. Griffin^a, David F. Tate^d, Ryan P. Cabeen^g, David H. Laidlaw^e, Thomas E. Conturo^f, Jacob D. Bolzenius^d, and Robert H. Paul^{a,d}

^aUniversity of Missouri- St. Louis, Department of Psychological Sciences, 1 University Blvd., Stadler Hall, St. Louis, MO 63121, United States

^bNeuroscience Research Australia, Barker Street Randwick, Sydney NSW 2031, Australia

^cSchool of Medical Sciences, University of New South Wales, Sydney NSW 2052, Australia

^dMissouri Institute of Mental Health, Berkeley, 4633 World Parkway Circle, Berkeley, MO 63134-3115, United States

^eBrown University, Computer Science Department, Providence, RI 02912, United States

^fWashington University School of Medicine, Mallinckrodt Institute of Radiology, 510 S. Kingshighway, St. Louis, MO 63110, United States

^gUniversity of Southern California, Keck School of Medicine, Los Angeles, CA 90032, United States

Abstract

Oxidative stress is a key mechanism of the aging process that can cause damage to brain white matter and cognitive functions. Polymorphisms in the superoxide dismutase 2 (*SOD2*) and catalase (*CAT*) genes have been associated with abnormalities in antioxidant enzyme activity in the aging brain, suggesting a risk for enhanced oxidative damage to white matter and cognition among older individuals with these genetic variants. The present study compared differences in white matter microstructure and cognition among 96 older adults with and without genetic risk factors of *SOD2* (rs4880) and *CAT* (rs1001179). Results revealed higher radial diffusivity in the anterior thalamic radiation among *SOD2* CC genotypes compared to CT/TT genotypes. Further, the CC genotype moderated the relationship between the hippocampal cingulum and processing speed, though this did not survive multiple test correction. The *CAT* polymorphism was not associated with brain outcomes in this cohort. These results suggest that the CC genotype of *SOD2* is an important genetic marker of suboptimal brain aging in healthy individuals.

Correspondence to: Lauren E. Salminen.

¹Present Address: University of Southern California, Imaging Genetics Center, Mark and Mary Neuroimaging and Informatics Institute, 4676 Admiralty Way, 2nd Floor, Marina del Rey, CA, 90292, United States.

All authors declare no conflicts of interest.

Keywords

Brain aging; Oxidative stress; *SOD2*; Catalase; White matter; Cognition

1. Introduction

Oxidative stress is a pathological mechanism of brain aging that involves an imbalance in the production and detoxification of reactive oxygen species (ROS) [1]. While modest levels of ROS are required to facilitate long-term potentiation (LTP) and synaptic plasticity [2,3], overproduction of ROS can cause damage to proteins, lipids, and mitochondrial DNA (mtDNA). Such damage impairs basic cellular processes including acetylcholine release, LTP, and saltatory conduction [4,5], which are critical for maintaining normal cognitive function in domains of executive function, processing speed, and memory [6].

Dysregulated ROS also damage the cellular architecture of the brain, with oligodendrocytes demonstrating enhanced vulnerability to ROS accumulation compared to other brain cells [7]. Age-related intracellular oxidation is enhanced in brain regions with an abundance of late-differentiating oligodendrocytes [4,8]. In contrast to early-differentiating oligodendrocytes that myelinate large diameter axons, late-differentiating oligodendrocytes have a “weaker” lipid profile that produces thinner myelin sheaths for many small diameter axon segments [9]. These small diameter axon fibers myelinate later in life and are believed to be the first to decline in older age due to their thin myelin sheaths [10,11]. Thinner myelin sheaths are predominantly located in intra-cortical association areas involved in higher-order cognitive integration [4,8]. White matter fiber tracts traversing these brain regions (i.e., white matter association tracts) are at increased risk for oxidative damage, which may result in cognitive difficulties [4,12].

Damage to white matter fiber tracts can be measured non-invasively using diffusion tensor imaging (DTI). DTI calculates the directional properties of water diffusion within an image voxel and can provide detailed information about underlying anatomy [13–15]. Fractional anisotropy (FA) and mean diffusivity (MD) are commonly used scalar metrics of white matter integrity. FA measures the degree of directional water restriction that is indicated by axonal fiber density and coherence [16]. Conversely, MD measures the average rate of water diffusion within a voxel that is determined by the density of anatomical barriers (e.g., myelin sheaths) and the exchange of water molecules between cellular compartments [16,17]. Axial diffusivity (AD) and radial diffusivity (RD) are two vector metrics that characterize the directionally dependent rate of water diffusion that occurs parallel and perpendicular to axon fibers, respectively [18]. Although multiple patterns of white matter diffusion have been reported in advanced age [19,20], the majority of studies using DTI scalar and vector metrics report decreased FA and increased MD, AD and RD [18–23]. This pattern of change typically occurs along an anterior to posterior gradient [20,24–28] and is believed to result from predominant demyelination and myelin loss.

Antioxidant defense enzymes are essential for combating oxidative stress and preventing damage to white matter microstructure. Superoxide dismutase (SOD) and catalase (CAT) are two of the most critical first-line antioxidant defense mechanisms against ROS in the human

brain [6]. SOD and CAT work synergistically to ameliorate the neurotoxic effects of oxidative stress by reducing ROS to less harmful compounds. Suboptimal concentrations of these enzymes in the brain limit the ability to combat the large quantities of highly reactive polyunsaturated fatty acids, iron, and ROS that accumulate with age [29]. Accordingly, genetic polymorphisms within the genes that encode SOD2 and CAT have been associated with numerous disorders involving oxidative stress. Specifically, the C allele (Ala) of the *SOD2* missense polymorphism, rs4880 (p.Val16Ala) has been associated with neurodegenerative diseases including Alzheimer's disease [30], Parkinson's disease [31], and sporadic motor neuron disease [32], and psychiatric conditions such as schizophrenia [33]. Less is known about the relationship between the *CAT*-262C > T polymorphism (rs1001179) and brain health, yet evidence suggests that the common C allele poses a greater risk for oxidative damage in the central nervous system (CNS) than the minor T allele. Specifically, the T allele has shown to protect against the development of diabetic neuropathy [34,35], acoustic neuroma [36], and neurological manifestations of Wilson's disease [37] compared to the C allele.

To date no studies have used DTI to examine relationships between genetic markers of oxidative stress and white matter integrity in normal aging, yet numerous studies acknowledge that oxidative stress is a likely driver of age-related changes in late-myelinating white matter pathways (i.e., retrogenesis). This represents a critical gap in the literature as oxidative damage to white matter tracts that innervate association brain regions may underlie cognitive variability among older individuals. The purpose of this study was to determine the impact of genetic risk factors of oxidative damage on white matter integrity and cognition using DTI metrics and neuropsychological indices. We hypothesized that individuals with genetic risk variants of *SOD2* and *CAT* would exhibit enhanced white matter damage in late-myelinating fiber tracts and cognitive difficulties in executive function, memory, and processing speed compared to individuals without these risk factors.

2. Method

2.1. Participants

Data were examined in 96 English-speaking older adults participating in an ongoing study of cognitive aging (R01-NS052470). Neuropsychological data, participant demographics and relevant health histories were obtained at the University of Missouri in St. Louis and neuroimaging was completed in a subset of these individuals (n = 71) at Washington University within one month of the neuropsychological visit for the majority of participants. All study protocols were approved by the IRB of these institutes. Participants provided informed consent and received financial compensation for their involvement in the study.

Individuals were excluded based on a self-reported history of a substance use disorder, psychiatric diagnosis (all Axis I and II disorders with the exception of treated depression), learning disability, any medical or neurological condition capable of impacting cognition (e.g., thyroid disease), history of head injury (defined by a loss of consciousness > 30 min), history of treatment-dependent diabetes, and contraindications for MRI (e.g., claustrophobia). Participants were required to independently complete basic and instrumental daily functions according to the Lawton and Brody Activities of Daily Living

scale (ADLs) [38], and receive a score ≥ 24 on the Mini Mental State Examination [39] to exclude individuals with probable dementia. MRI scans were inspected by a radiologist and individuals demonstrating clinically significant abnormalities (e.g., normal pressure hydrocephalus) were excluded from the study and instructed to contact their primary care physician.

2.2. Genotyping

Genetic isolation and processing was completed at Genetics Repositories Australia. Genomic DNA was extracted from saliva samples using the Oragene DNA collection kit (DNA Genotek, Ottawa, Canada) and the Autopure LS nucleic acid purification system (QIAgen). Genotypes for *SOD2* and *CAT* were ascertained using predesigned Taqman SNP Genotyping Assays (Applied Biosystems) according to the manufacturer's protocol: *SOD2* rs4880 (Assay ID C_8709053_10) *CAT*-262 rs1001179 (Assay ID C_11468118_10).

The following allele frequencies were observed: *SOD2*: CC n = 26, CT n = 43, TT n = 27; *CAT*: CC n = 61, CT n = 32, TT n = 3. Genotype frequencies for both SNPs did not deviate from Hardy-Weinberg equilibrium (rs4880, $\chi^2 = 1.04$, df = 1, p = 0.308; rs1001179, $\chi^2 = 0.24$, df = 1, p = 0.064). Given the cell sizes for *CAT*, a dominant grouping system was used to compare individuals with the CC genotype against individuals with the CT/TT genotypes. While these genotypes are arranged according to a recessive grouping system, this model is functionally dominant as the C allele is far more common than the minor T allele and thus is inferred to have the dominant effect. For *SOD2*, preliminary analyses indicated that the recessive model was the most robust to brain outcomes in this study. Thus, individuals with the CC genotype of *SOD2* were compared against individuals with the CT/TT genotypes.

2.3. Imaging acquisition and analysis

All imaging acquisition was performed using a head-only Magnetom Allegra 3T MRI scanner (Siemens Medical Solutions, Erlangen, Germany) located at Washington University. This high performance scanner has gradients with a maximum strength of 40 mT/m in a 100 μ s rise time and a slew rate of 400/T/m/s, with 100% duty cycle. Acquisition parameters were designed for whole-brain coverage, high signal-to-noise ratio (SNR), and minimal artifact. Subject head movement was restrained using specialized foam pads and the application of surgical tape across the forehead. An initial scout scan consisting of three orthogonal planes was obtained at the beginning of each scanning session to confirm head position. Daily quality assurance tests were performed to ensure consistent scanner performance across subjects. The same scanner, operating system and processing software were used throughout the duration of the study. Total scan time was < 1 h. Standard shimming was applied.

Axial diffusion-weighted images (DWIs) were obtained with a custom single-shot multislice echo-planar tensor encoded pulse sequence with diffusion-encoding gradients applied in 31 non-collinear directions and 24 main directions ($b = 996$ s/mm²). To maximize SNR and directional coverage we used a "core" of tetrahedral-perpendicular directions ($b = 1412$ and 680 s/mm²) with 5 I0 acquisitions ($b \sim 0$) [40]. The following pulse sequence parameters were also implemented: TE = 86.2 ms; TR = 7.82 s; 64 contiguous 2.0-mm slices; and an

acquisition matrix of 128×128 with a FOV of 256×256 mm (isotropic $2.0 \times 2.0 \times 2.0$ mm voxels). A total of 72 acquisitions were averaged over 2 scan repeats.

Brain tissue was extracted using the FSL Brain Extraction Tool and diffusion-weighted volume was corrected for subject motion and artifacts by affine registration using FSL FLIRT [41]. Linear least squares and trilinear interpolation was used to reconstruct the diffusion tensors of the DWI signal [42]. Individual tracts were identified using deterministic whole-brain streamline tractography with one randomly placed seed per voxel, second-order Runge-Kutta integration, a 35° flip angle, FA of 0.15, and minimum fiber length of 10 mm. Each participant's FA image was registered to the Johns Hopkins University (JHU) white matter atlas using FSL FLIRT with mutual information. Tracts of interest included white matter association tracts such as the superior longitudinal fasciculus (SLF), inferior longitudinal fasciculus (ILF), inferior fronto-occipital fasciculus (IFOF), uncinate fasciculus (UF), and cingulum bundle [43]. Although not classically defined as an association tract, we also examined the anterior thalamic radiation (ATR), as this tract innervates association areas and has been previously associated with brain aging and decline in executive function, processing speed, and memory [44–46]. Each tract was modeled separately by hemisphere for a total of 12 distinct tracts. As described in the statistical analysis section below, tracts were collapsed across hemispheres to provide an average measure of FA, MD, AD, and RD for each fiber bundle. The JHU atlas was used to determine which streamlines would be included in a specific bundle. Streamlines were retained in the bundle if at least 80% of fiber arc length was included in the bundle mask. Streamlines that came within .8 mm of an existing tract were removed from the analysis [47]. Numerical integration was used to compute average scalar and vector values along each streamline, and average FA, MD, AD, and RD for each bundle was computed for the streamline measures.

2.4. Neuropsychological assessment

All participants completed a comprehensive neuropsychological evaluation at the University of Missouri in St. Louis. Demographic information and health histories were obtained via self-report questionnaires. Blood pressure was measured at three time points during the cognitive visit to account for the potential influence of hypertension on cognitive performance. The neuropsychological tests were chosen based on established sensitivity to age-related cognitive decline. This study focused on cognitive domains of processing speed, executive function, and memory, as previous research suggests that these functions may be influenced by age-related increases in oxidative stress. Cognitive difficulties in these domains have also been linked to alterations in white matter association tracts and the ATR. Composite scores for each cognitive domain were used as the primary outcome measures for the neuropsychological variables to facilitate data reduction. In order to determine composite scores, raw scores from each cognitive test were converted to z scores and averaged for each domain. Scores measured in completion time were multiplied by -1 to result in all positive integers.

The cognitive battery consisted of the following tests: Processing speed: 1) Trails A from the Trail Making Test [48], 2) Trial 1 from the Color-Word Interference Task (CWIT) of the Delis-Kaplan Executive Function System [49], and 3) Coding from the Repeatable Battery

for the Assessment of Neuropsychological Status [50]; Executive function: 1) Trails B from the Trail Making Test, 2) Trial 4 from the CWIT, and 3) Letter Number Sequencing (LNS) from the Wechsler Adult Intelligence Scale-III [51]; Memory: list learning, story memory, list recall, and story recall from the RBANS. Time to completion was the primary outcome measure for the Trail Making Test and CWIT. All other tests were measured by the total number of correct responses.

2.5. Statistical analyses

Chi square and independent samples t-tests were used to examine group differences in sex, race, age, and years of education (respectively). Group differences in descriptive variables such as hypertension (systolic blood pressure ≥ 140 mmHg or diastolic ≥ 90 mmHg), intracranial volume (ICV) were also examined. Variables that differed significantly ($p < .05$) between groups and were significantly correlated with the dependent variables were included as covariates in the main analyses to control for any intervening effects on the outcome measures. Statistical significance was initially determined using an alpha level of .05. False Discovery Rate (FDR) corrections were implemented to control for type 1 error.

Separate multivariate analysis of variance (MANOVA) models were used to examine the impact of *SOD2* and *CAT* on white matter integrity. Genetic status served as the independent variable and white matter tracts served as the dependent variables in each MANOVA. Outcomes from each DTI metric were analyzed in separate MANOVAs to minimize metric-specific variance. Separate ANOVA models were used to examine the impact of *SOD2* and *CAT* on the three cognitive domain scores (processing speed, executive function, and memory). We examined domain scores separately due to potential differences in the sensitivity of each domain to discriminate between groups. Genetic status served as the independent variable and cognitive domain scores served as the dependent variable in each analysis. Multiple regression models were computed to determine the relationship between tract-specific DTI metrics (X_1) on cognitive domain scores (Y), and to determine whether an interaction between genetic status (X_2) and DTI metrics moderated these relationships ($X_1 * X_2$); $Y_i = \beta_0 + \beta_1 X_{1i} + \beta_2 X_{2i} + \beta_3 X_{1i} * X_{2i} + \epsilon_i$. To reduce multicollinearity, DTI metrics and genetic status (e.g., *SOD2*) were mean-centered prior to calculation of the interaction terms. Given a priori evidence of associations between the selected tracts and cognition, we applied FDR corrections (q) separately to the main effects and interactions ($7 \text{ tracts} \times 3 \text{ domains} \times 3 \text{ DTI metrics} = 63 \text{ comparisons}$).

3. Results

3.1. Data screening and preliminary analyses

Q-Q plots and boxplots revealed abnormal performance scores for one subject, and removal of this subject yielded a normal distribution for each cognitive domain. Normality tests indicated that RD and AD values were leptokurtic and positively skewed beyond the acceptable range. A log10 transformation was then applied to all RD and AD values. While skewness and kurtosis improved, Q-Q plots and boxplots revealed extreme scores ($> 3 \times$ interquartile range) for one subject across multiple tracts. This subject was removed from all analyses and the shape of the distribution was normalized. Pearson's R revealed very strong

correlations (r 's $> .8$) between MD and RD for nearly all tracts, and thus MD was dropped from the analysis to reduce redundancy in the outcomes. RD was retained (versus MD) due to its enhanced sensitivity to demyelination and suggestions that MD changes are driven by changes in RD [52,53]. Pillai's Trace was used for MANOVAs that violated statistical assumptions (Box's $M < .001$, Bartlett's test $> .001$, Levene's test $< .05$) [54]. Descriptive variables did not differ between the CC ($n = 26$) and CT/TT ($n = 68$) genotypes of *SOD2* or the CC/CT ($n = 60$) and TT ($n = 34$) genotypes of *CAT* (Table 1). As such, covariates were not utilized in the main analyses.

3.2. Multivariate effects of SOD2 and CAT

A significant multivariate main effect was observed for RD (Pillai's Trace = 0.243, $F(7,58) = 2.67$, $p = 0.018$, $f^2 = 0.32$), with the CC group demonstrating significantly higher RD ($p = .001$) in the ATR compared to the CT/TT group (Fig. 1A). Groups did not differ significantly for AD (Pillai's Trace = 0.172, $F(7,58) = 1.72$, $p = 0.122$, $f^2 = 0.21$) or FA (Wilks' $\Lambda = 0.870$, $F(7,58) = 1.24$, $p = 0.295$, $f^2 = 0.15$). No significant differences were observed for processing speed ($F(1,88) = .07$, $p = 0.791$, $f = .03$), executive function ($F(1,86) = .30$, $p = 0.588$, $f = .05$), or memory ($F(1,92) = .67$, $p = 0.415$, $f = .08$). RD in the ATR remained statistically significant ($p < .002$) after applying FDR corrections to the univariate results.

Significant multivariate effects were not observed for FA (Wilks' $\Lambda = 0.926$, $F(7,58) = .66$, $p = 0.701$, $f^2 = 0.08$), RD (Wilks' $\Lambda = 0.904$, $F(7,58) = .88$, $p = 0.527$, $f^2 = 0.12$), or AD (Wilks' $\Lambda = 0.822$, $F(7,58) = 1.79$, $p = 0.107$, $f^2 = 0.22$). Groups did not differ significantly on processing speed ($F(1,88) = .00$, $p = 0.981$, $f < .001$), executive function ($F(1,86) = .02$, $p = 0.903$, $f < .001$), and memory ($F(1,92) = .00$, $p = 0.953$, $f < .001$). Given the lack of significant effect of this SNP on the outcome measures, only *SOD2* was tested as a moderating variable between white matter tracts and cognition.

3.3. Relationships between white matter tracts and cognition by SOD2

Statistical results of significant (FDR adjusted q) and trending ($p < .05$) main effects are presented in Table 2. All significant DTI \times cognition relationships were observed at $q < .013$. For processing speed, significant main effects were observed with FA in the ILF and IFOF; AD in the SLF, IFOF, CGC, ATR, and UF; and RD in the ILF, IFOF, SLF, CGC, ATR, and UF. Lower FA and higher AD and RD in these tracts was associated with slower processing speed. For executive function, we observed significant main effects for FA in the ILF and IFOF, with lower FA predicting poorer performance on executive tasks. Trend effects were also observed for AD in the SLF, ATR, and UF; and RD in the ILF, IFOF, and CGC (Table 2). Here, higher AD and RD was associated with worse performance. For memory, we did not observe significant main effects after the FDR correction, though a trend was observed for lower FA in the ILF and worse memory recall.

We did not observe significant interactions between white matter tracts and *SOD2* on cognition after correcting for multiple comparisons. However, we did observe noteworthy trends between RD in the CHC and *SOD2* ($F(3,60) = 3.37$, $p = 0.024$), and FA in the CGC and *SOD2* ($F(3,63) = 3.06$, $p = 0.035$) on processing speed. In the CHC, the interaction between RD and *SOD2* uniquely explained 12% of the variance in processing speed (semi-

partial $r = .345$). Simple slope analyses revealed a negative relationship between RD in the CHC and slower processing speed in CC genotypes ($t = -3.12$, $p = .003$), but this was not observed in CT/TT genotypes ($t = .32$, $p = .747$; Fig. 2A). For the CGC, 6% of the variance in processing speed could be explained by the interaction between FA and *SOD2* (semi-partial $r = -.261$). Simple slopes also revealed a positive relationship between FA in the CGC and processing speed among CC genotypes ($t = 2.87$, $p = .006$), but this was not observed in CT/TT genotypes ($t = .69$, $p = .492$; Fig. 2B).

4. Discussion

The present study is the first to examine the influence of antioxidant defense genes on brain white matter and cognition in a healthy sample of older individuals. Results revealed higher RD in the ATR of individuals with the CC genotype of *SOD2* compared to those with the CT and TT genotypes. Group differences in RD were also evident in the CGC, though this finding did not survive the FDR correction. Although moderation effects also did not survive FDR, we did observe trend effects for higher RD in the CHC and slower processing speed in CC genotypes. In contrast to *SOD2*, genetic variants of the *CAT* polymorphism were not related to white matter or cognition in this cohort. Collectively these results provide preliminary evidence that the CC genotype of *SOD2* is a risk factor for microstructural white matter damage and associated reductions in processing speed in otherwise healthy older adults.

Structural alterations in the ATR and cingulum have been reported in previous studies of brain aging [44,45,55,56], Alzheimer's disease [57–59], Parkinson's disease [60,61], and schizophrenia [62,63], among others. Oxidative stress is implicated in the pathogenesis of these conditions, which is consistent with studies reporting an increase risk for Alzheimer's disease, Parkinson's disease, and schizophrenia among CC genotypes of *SOD2*/rs4880 [30–33]. In the present study we show that the ATR, and to a lesser extent the cingulum, are at increased risk for degradation in non-clinical older persons with the *SOD2* CC genotype. The ATR and cingulum are prominent white matter tracts that include connection sites with the prefrontal cortex (PFC), cingulate cortex, and thalamic nuclei [64,65]. Fiber dissection techniques and DTI tractography studies show that the ATR and cingulum are fiber bundles within the Papez circuit [66,67], which is a limbic system pathway involved in emotional expression and memory [68]. Neuro-transmitter signaling within the Papez circuit is primarily excitatory [69], causing ROS production via NMDA receptor activation [70,71]. NMDA receptors are located in oligodendrocytes and myelin sheaths, and have shown to become activated in response to neuronal injury [72,73]. Thus, upregulated NMDA activation in damaged brain tissue and corresponding increases in ROS production can deplete the already limited stores of cellular antioxidants in the aging brain, ultimately leading to perpetuated mitochondrial dysfunction, glutamate neuro-toxicity, and cell death [74]. It is possible that older individuals with the CC genotype of *SOD2* have increased difficulty for detoxifying ROS in the Papez circuit due to limited levels of *SOD2*. Although this remains conjecture at this point, imaging modalities such as positron emission tomography (PET) would be useful for clarifying relationships between *SOD2* genetic status and in vivo glutamate and NMDA receptor binding within regions of the Papez circuit.

RD was the most robust DTI metric to genetic differences in *SOD2*, which is consistent with the hypothesis that oxidative stress is detrimental to myelin integrity. RD is believed to be preferentially sensitive to changes in the myelin sheath compared to other DTI metrics. Work by Song et al. [53,75] demonstrated that RD could distinguish demyelination from axonal damage in mouse models of retinal ischemia and multiple sclerosis. Additional work from Nair et al. [76] revealed increased RD in mice that were genetically modified to be myelin-deficient, which corresponds to the positive correlation between RD and demyelination severity observed in human post mortem tissue samples of multiple sclerosis patients [77]. In vivo studies of human brain aging reveal various patterns of diffusivity that are expected to reflect different mechanisms of neuropathology [19,20], with FA and AD more closely linked to axonal damage and MD and RD linked to demyelination. Decreased FA and increased RD is commonly observed in white matter tracts traversing the frontal lobe during normal aging [78], supporting the theory that the increased metabolic activity of oligodendrocytes in late-myelinating association pathways makes them more vulnerable to oxidative damage. Madden et al. [78] noted that a concurrent decrease in FA and increase in RD likely represents pathology of both the axon and myelin sheath. Although brain aging affects both axonal and myelin integrity, results from our study suggest that genetic differences in *SOD2* specifically influences myelin disruption in healthy older adults.

The lack of cognitive differences between *SOD2* groups may be due to the relatively young age of the sample ($M_{age} = 63$ years). Previous research by Tucker-Drob and Briley [79] demonstrated that approximately one third of between-subject variability in cognitive changes between ages 65–96 is explained by genetic differences, whereas no cohesive pattern of indicators could explain the variability in cognitive aging between ages 50–65. This is in agreement with the resource-modulation hypothesis, which theorizes that increased depletion of brain resources modulates the impact of common genetic variants on cognition, and therefore the impact of such variants becomes more significant with advanced age [80]. Many studies show support for this model by revealing modest or non-existent genetic effects in young adults relative to older adults [81]. Additional studies are needed in a slightly older cohort to determine whether there is an age-dependent relationship between *SOD2* and cognition.

Despite the absence of a direct effect of *SOD2* on cognitive function, the CC genotype moderated the relationship between the cingulum and processing speed, with a stronger interaction in the CHC compared to the CGC. Interestingly, previous research shows that alterations in the CHC are more closely linked to pathological aging and Alzheimer's disease compared to alterations in the CGC [82–86]. Accordingly, Laukka et al. [87] revealed weaker associations between age-related changes in the CHC and reduced processing speed when cognitively “normal” older adults were excluded for prodromal dementia (assessed retrospectively from longitudinal follow up). The CHC is a fiber pathway within the Papez circuit that connects the posterior cingulate cortex (PCC) with the medial temporal lobe [88], the latter of which harbors the hippocampal region, entorhinal, and parahippocampal cortices. Each of these structures is vulnerable to Alzheimer's pathology, particularly the accumulation of oxidative end products and reduced antioxidant capacity in the hippocampus. Both aging and genetically determined *SOD2* deficiencies promote oxidative stress in the hippocampus, thereby leading to reductions in cognitive function [89].

Relatedly, the PCC is a primary connectivity hub for major cortical networks [90], allowing information processing across disparate brain systems. Disrupted functional connectivity of the PCC has been associated with reduced processing speed in aging individuals [91,92], which may explain the link between the increased RD in the CHC and slower processing speed in CC genotypes of *SOD2*. Given the strong biological rationale for this effect, it is likely that cingulum moderations did not survive multiple test correction due to low power, rather than being a spurious result.

In contrast to our hypotheses, *CAT* was not significantly related to white matter or cognition in this cohort of individuals. Although this was unexpected, previous research has reported conflicting results regarding the impact of this SNP on various health conditions. Some studies show that the minor T allele is protective against diabetic neuropathy, acoustic neuroma, and later presentation of neurological manifestations of Wilson's disease [34–37], while other studies report an increase risk for breast and prostate cancer [93,94], chronic hepatitis B [95], alcohol dependency [96], ulcerative colitis [97], and asthma [98,99]. Additional research investigations have reported no association between *CAT* and sporadic Alzheimer's disease [100], hypertension [101], and depression [102]. Forseberg et al. [103] revealed differences in allelic expression across organ tissues, which may explain the discrepancy of allelic risk in the abovementioned studies. Future studies conducted in larger samples should examine potential pleiotropic effects of the *CAT* polymorphism, as well as interactions with other genes.

The results of this study should be regarded as preliminary, due to the limited cell sizes of the genetic groups. However, the strong biological model and reported effect sizes suggest that our results reflect a true effect of the *SOD2* polymorphism on brain aging. Nevertheless, replication is needed in a larger sample to confirm our findings. A few other limitations should be acknowledged. First, this study did not include a plasma or cerebrospinal fluid biomarker of oxidative stress or antioxidant enzyme activity and therefore the functional impact of *SOD2* and *CAT* on brain microphysiology remains unknown. While previous studies have measured antioxidant activity from plasma and serum, the relationship between central and peripheral levels of enzyme activity is not consistent [29]. Second, the use of AD and RD is controversial due to potential misinterpretations of what is truly axonal degeneration versus demyelination [78,104]. Interpretation that increased RD in the present study represents demyelination is based on previously identified patterns of DTI changes that correspond to histological data [19]. While it is possible that increased RD in the ATR also reflects axonal damage given the established correlations between demyelination and axonal degeneration [77], the weight of literature regarding diffusivity patterns and oxidative mechanisms suggests that RD changes were likely driven by demyelination. Neuro-pathological data are required to address this hypothesis. Third, participants were recruited using advertisements for “healthy cognitive aging” and as such there may have been a sampling bias for individuals who were already concerned about their cognitive health. While a sampling bias may have influenced the level of cognitive performance exhibited by this cohort as a whole, it is unlikely that this would have influenced genetic differences in brain outcomes. Finally, this sample has been subject to previous genotype-phenotype analysis and therefore caution is warranted when interpreting the results.

5. Conclusion

The work presented herein is highly innovative as it is the first *in vivo* examination of brain outcomes among healthy older adults with genetic risk variants of *SOD2* and *CAT*. While our results do not support a role for *CAT* in “normal” brain aging, the CC genotype of *SOD2* appears to confer risk for tract-specific alterations in the Papez circuit that are related to slower processing speed. Knowledge of these associations should facilitate research aimed at developing intervention strategies for individuals at risk for *SOD2* deficiencies, whether by exogenous antioxidant supplementation or modification of lifestyle factors that reduce the burden of oxidative stress in the aging brain. Future studies utilizing PET imaging will further elucidate the relationship between *SOD2* and metabolic disturbances in the Papez circuit, particularly in the ATR and cingulum. Longitudinal studies examining a slightly older cohort (age 65) will be beneficial for determining the degree to which these antioxidant defense genes influence intra-individual variability in normal brain aging.

Acknowledgments

This work was supported by the National Institutes of Health (NIH)/National Institute on Aging [5F31AG050450]; NIH/National Institute of Neurological Disorders and Stroke [R01NS052470, R01NS039538]; the NIH/National Institute of Mental Health [R21MH090494]; and the Australian National Health and Medical Research Council [1037196]. Recruitment database searches were supported in part by the NIH/National Center for Research Resources [UL1 TR000448].

References

1. Hensley K, Robinson KA, Gabbita SP, Salsman S, Floyd RA. Reactive oxygen species, cell signaling, and cell injury. *Free Radical Biol Med*. 2000; 28(10):1456–1462. [PubMed: 10927169]
2. Kishida KT, Klann E. Sources and targets of reactive oxygen species in synaptic plasticity and memory. *Antioxid Redox Signal*. 2007; 9(2):233–244. [PubMed: 17115936]
3. Serrano F, Klann E. Reactive oxygen species and synaptic plasticity in the aging hippocampus. *Ageing Res Rev*. 2004; 3(4):431–443. [PubMed: 15541710]
4. Bartzokis G. Age-related myelin breakdown: a developmental model of cognitive decline and Alzheimer's disease. *Neurobiol Aging*. 2004; 25(1):5–18. [PubMed: 14675724]
5. Watson JB, Arnold MM, Ho YS, O'Dell TJ. Age-dependent modulation of hippocampal long-term potentiation by antioxidant enzymes. *J Neurosci Res*. 2006; 84(7):1564–1574. [PubMed: 16941635]
6. Salminen LE, Paul RH. Oxidative stress and genetic markers of suboptimal antioxidant defense in the aging brain: a theoretical review. *Rev Neurosci*. 2014; 25(6):805–819. [PubMed: 25153586]
7. LeDoux SP, Shen CC, Grishko VI, Fields PA, Gard AL, Wilson GL. Glial cell-specific differences in response to alkylation damage. *Glia*. 1998; 24(3):304–312. [PubMed: 9775981]
8. Bartzokis G, Beckson M, Lu PH, Nuechterlein KH, Edwards N, Mintz J. Age-related changes in frontal and temporal lobe volumes in men: a magnetic resonance imaging study. *Arch Gen Psychiatry*. 2001; 58(5):461–465. [PubMed: 11343525]
9. Wood, P., Bunge, RP. *Oligodendroglia*. Springer; US: 1984. The biology of the oligodendrocyte; p. 1-46.
10. Pakkenberg B, Pelvig D, Marner L, Bundgaard MJ, Gundersen HJG, Nyengaard JR, Regeur L. Aging and the human neocortex. *Exp Gerontol*. 2003; 38(1):95–99. [PubMed: 12543266]
11. Tang Y, Nyengaard JR, Pakkenberg B, Gundersen HJG. Age-induced white matter changes in the human brain: a stereological investigation. *Neurobiol Aging*. 1997; 18(6):609–615. [PubMed: 9461058]
12. Bartzokis G, Cummings JL, Sultzer D, Henderson VW, Nuechterlein KH, Mintz J. White matter structural integrity in healthy aging adults and patients with Alzheimer disease: a magnetic resonance imaging study. *Arch Neurol*. 2003; 60(3):393–398. [PubMed: 12633151]

13. Basser PJ, Pierpaoli C. Microstructural and physiological features of tissues elucidated by quantitative-diffusion-tensor MRI. *J Magn Res.* 2011; 213(2):560–570.
14. Conturo TE, Lori NF, Cull TS, Akbudak E, Snyder AZ, Shimony JS, Raichle ME. Tracking neuronal fiber pathways in the living human brain. *Proc Natl Acad Sci.* 1999; 96(18):10422–10427. [PubMed: 10468624]
16. Beaulieu C. The basis of anisotropic water diffusion in the nervous system—a technical review. *NMR Biomed.* 2002; 15(7-8):435–455. [PubMed: 12489094]
17. Sen PN, Basser PJ. A model for diffusion in white matter in the brain. *Biophys J.* 2005; 89(5):2927–2938. [PubMed: 16100258]
18. Alexander AL, Lee JE, Lazar M, Field AS. Diffusion tensor imaging of the brain. *Neurotherapeutics.* 2007; 4(3):316–329. [PubMed: 17599699]
19. Burzynska AZ, Preuschhof C, Bäckman L, Nyberg L, Li SC, Lindenberger U, Heekeren HR. Age-related differences in white matter microstructure: region-specific patterns of diffusivity. *Neuroimage.* 2010; 49(3):2104–2112. [PubMed: 19782758]
20. Bennett IJ, Madden DJ, Vaidya CJ, Howard DV, Howard JH. Age-related differences in multiple measures of white matter integrity: a diffusion tensor imaging study of healthy aging. *Hum Brain Map.* 2010; 31(3):378–390.
21. Lebel C, Gee M, Camicioli R, Wieler M, Martin W, Beaulieu C. Diffusion tensor imaging of white matter tract evolution over the lifespan. *Neuroimage.* 2012; 60(1):340–352. [PubMed: 22178809]
22. Sexton CE, Walhovd KB, Storsve AB, Tamnes CK, Westlye LT, Johansen-Berg H, Fjell AM. Accelerated changes in white matter microstructure during aging: a longitudinal diffusion tensor imaging study. *J Neurosci.* 2014; 34(46):15425–15436. [PubMed: 25392509]
23. Westlye LT, Walhovd KB, Dale AM, Bjørnerud A, Due-Tønnessen P, Engvig A, et al. Life-span changes of the human brain white matter: diffusion tensor imaging (DTI) and volumetry. *Cereb Cortex.* 2009; 20(9):2055–2068. [PubMed: 20032062]
24. Head D, Buckner RL, Shimony JS, Williams LE, Akbudak E, Conturo TE, et al. Differential vulnerability of anterior white matter in nondemented aging with minimal acceleration in dementia of the Alzheimer type: evidence from diffusion tensor imaging. *Cereb Cortex.* 2004; 14(4):410–423. [PubMed: 15028645]
25. O'Sullivan MRC, Jones DK, Summers PE, Morris RG, Williams SCR, Markus HS. Evidence for cortical disconnection as a mechanism of age-related cognitive decline. *Neurology.* 2001; 57(4):632–638. [PubMed: 11524471]
26. Pfefferbaum A, Sullivan EV, Hedehus M, Lim KO, Adalsteinsson E, Moseley M. Age-related decline in brain white matter anisotropy measured with spatially corrected echo-planar diffusion tensor imaging. *Magn Reson Med.* 2000; 44(2):259–268. [PubMed: 10918325]
27. Pfefferbaum A, Adalsteinsson E, Sullivan EV. Frontal circuitry degradation marks healthy adult aging: evidence from diffusion tensor imaging. *Neuroimage.* 2005; 26(3):891–899. [PubMed: 15955499]
28. Salat DH, Tuch DS, Greve DN, Van Der Kouwe AJW, Hevelone ND, Zaleta AK, Dale AM. Age-related alterations in white matter microstructure measured by diffusion tensor imaging. *Neurobiol Aging.* 2005; 26(8):1215–1227. [PubMed: 15917106]
29. Reiter RJ. Oxidative processes and antioxidative defense mechanisms in the aging brain. *FASEB J.* 1995; 9(7):526–533. [PubMed: 7737461]
30. Wiener HW, Perry RT, Chen Z, Harrell LE, Go RCP. A polymorphism in SOD2 is associated with development of Alzheimer's disease. *Genes Brain Behav.* 2007; 6(8):770–776. [PubMed: 17376152]
31. Shimoda-Matsubayashi S, Matsumine H, Kobayashi T, Nakagawa-Hattori Y, Shimizu Y, Mizuno Y. Structural dimorphism in the mitochondrial targeting sequence in the human manganese superoxide dismutase gene: a predictive evidence for conformational change to influence mitochondrial transport and a study of allelic association in Parkinson's disease. *Biochem Biophys Res Commun.* 1996; 226(2):561–565. [PubMed: 8806673]
32. Landeghem GF, Tabatabaie P, Beckman G, Beckman L, Andersen PM. Manganese-containing superoxide dismutase signal sequence polymorphism associated with sporadic motor neuron disease. *Euro J Neurol.* 1999; 6(6):639–644.

33. Akyol O, Yanik M, Elyas H, Namli M, Canatan H, Akin H, et al. Association between Ala-9Val polymorphism of Mn-SOD gene and schizophrenia. *Prog Neuropsychopharmacol Biol Psychiatr*. 2005; 29(1):123–131.
34. Chistiakov DA, Zotova EV, Savost'yanov KV, Bursa TR, Galeev IV, Stokov IA, Nosikov VV. The 262T > C promoter polymorphism of the catalase gene is associated with diabetic neuropathy in type 1 diabetic Russian patients. *Diabetes Metab*. 2006; 32(1):63–68. [PubMed: 16523188]
35. Zotova EV, Savost'yanov KV, Chistyakov DA, Bursa TR, Galeev IV, Stokov IA, Nosikov VV. Association of polymorphic markers of the antioxidant enzyme genes with diabetic polyneuropathy in type 1 diabetes mellitus. *Mol Biol*. 2004; 38(2):200–204.
36. Rajaraman P, Hutchinson A, Rothman N, Black PM, Fine HA, Loeffler JS, et al. Oxidative response gene polymorphisms and risk of adult brain tumors. *Neuro-oncology*. 2008; 10(5):709–715. [PubMed: 18682580]
37. Gromadzka G, Kruszyhska M, Wierzbicka D, Litwin T, Dzieyc K, Wierchowska-Ciok A, et al. Gene variants encoding proteins involved in antioxidant defense system and the clinical expression of Wilson disease. *Liver Int*. 2015; 35(1):215–222. [PubMed: 24517502]
38. Lawton MP, Brody EM. Assessment of older people: self-maintaining and instrumental activities of daily living. *Gerontologist*. 1969; 9:179–186. [PubMed: 5349366]
39. Folstein MF, Folstein SE, McHugh PR. Mini-mental state: a practical method for grading the cognitive state of patients for the clinician. *J Psychiatr Res*. 1975; 12(3):189–198. [PubMed: 1202204]
40. Conturo TE, McKinstry RC, Akbudak E, Robinson BH. Encoding of anisotropic diffusion with tetrahedral gradients: a general mathematical diffusion formalism and experimental results. *Magn Res Med*. 1996; 35(3):399–412.
41. Jenkinson M, Bannister P, Brady M, Smith S. Improved optimization for the robust and accurate linear registration and motion correction of brain images. *Neuroimage*. 2002; 17(2):825–841. [PubMed: 12377157]
42. Zhukov L, Barr AH. Oriented tensor reconstruction: tracing neural pathways from diffusion tensor MRI. *Visualization*. 2002:387–394.
43. Jellison BJ, Field AS, Medow J, Lazar M, Salamat MS, Alexander AL. Diffusion tensor imaging of cerebral white matter: a pictorial review of physics, fiber tract anatomy, and tumor imaging patterns. *Am J Neuroradiol*. 2004; 25(3):356–369. [PubMed: 15037456]
44. Baker LM, Laidlaw DH, Conturo TE, Hogan J, Zhao Y, Luo X, et al. White matter changes with age utilizing quantitative diffusion MRI. *Neurology*. 2014; 83(3):247–252. [PubMed: 24928121]
45. Cremers LG, de Groot M, Hofman A, Krestin GP, van der Lugt A, Niessen WJ, et al. Altered tract-specific white matter microstructure is related to poorer cognitive performance: the Rotterdam Study. *Neurobiol Aging*. 2016; 39:108–117. [PubMed: 26923407]
46. Nishio Y, Hashimoto M, Ishii K, Ito D, Mugikura S, Takahashi S, Mori E. Multiple thalamo-cortical disconnections in anterior thalamic infarction: implications for thalamic mechanisms of memory and language. *Neuropsychologia*. 2014; 53:264–273. [PubMed: 24321272]
47. Zhang S, Demiralp C, Laidlaw DH. Visualizing diffusion tensor MR images using streamtubes and streamsurfaces. *IEEE Trans Vis Comput Graph*. 2003; 9(4):454–462.
48. Manual of Directions and Scoring. War Department, Adjutant General's Office; Washington, DC: 1944. Army Individual Test Battery.
49. Delis, DC., Kaplan, E., Kramer, JH. Delis-Kaplan Executive Function System (D-KEFS). Psychological Corporation; 2001.
50. Randolph, C. RBANS Manual: Repeatable Battery for the Assessment of Neuropsychological Status. The Psychological Corporation; San Antonio, TX: 1998.
51. Wechsler, D. WISC-III: Wechsler Intelligence Scale for Children: Manual. Psychological Corporation; 1991.
52. Lentz MR, Peterson KL, Ibrahim WG, Lee DE, Sarlls J, Lizak MJ, et al. Diffusion tensor and volumetric magnetic resonance measures as biomarkers of brain damage in a small animal model of HIV. *PLoS One*. 2014; 9(8):e105752. [PubMed: 25144656]

53. Song SK, Yoshino J, Le TQ, Lin SJ, Sun SW, Cross AH, Armstrong RC. Demyelination increases radial diffusivity in corpus callosum of mouse brain. *Neuroimage*. 2005; 26(1):132–140. [PubMed: 15862213]
54. Meyers, LS., Gamst, G., Guarino, AJ. *Applied Multivariate Research: Design and Interpretation*. Sage Publications; Thousand Oaks: 2006.
55. Gunbey HP, Ercan K, Fındıkoğlu AS, Bulut HT, Karaoglanoglu M, Arslan H. The limbic degradation of aging brain: a quantitative analysis with diffusion tensor imaging. *Sci World J*. 2014; 2014
56. Mella N, de Ribaupierre S, Eagleson R, De Ribaupierre A. Cognitive intraindividual variability and white matter integrity in aging. *Sci World J*. 2013; 2013
57. Aggleton JP, Pralus A, Nelson AJ, Hornberger M. Thalamic pathology and memory loss in early Alzheimer's disease: moving the focus from the medial temporal lobe to Papez circuit. *Brain*. 2016:aww083.
58. Hornberger M, Wong S, Tan R, Irish M, Piguet O, Kril J, et al. In vivo and postmortem memory circuit integrity in frontotemporal dementia and Alzheimer's disease. *Brain*. 2012; 135(10):3015–3025. [PubMed: 23012333]
59. Torso M, Serra L, Giulietti G, Spanò B, Tuzzi E, Koch G, et al. Strategic lesions in the anterior thalamic radiation and apathy in early Alzheimer's disease. *PLoS One*. 2015; 10(5):e0124998. [PubMed: 25932637]
60. Kamagata K, Motoi Y, Abe O, Shimoji K, Hori M, Nakanishi A, et al. White matter alteration of the cingulum in Parkinson disease with and without dementia: evaluation by diffusion tensor tract-specific analysis. *Am J Neuroradiol*. 2012; 33(5):890–895. [PubMed: 22241380]
61. Vercruyse S, Leunissen I, Vervoort G, Vandenberghe W, Swinnen S, Nieuwboer A. Microstructural changes in white matter associated with freezing of gait in Parkinson's disease. *Mov Disord*. 2015; 30(4):567–576. [PubMed: 25640958]
62. Ellison-Wright I, Nathan PJ, Bullmore ET, Zaman R, Dudas RB, Agius M, et al. Distribution of tract deficits in schizophrenia. *BMC Psychiatry*. 2014; 14(1):99. [PubMed: 24693962]
63. Whitford TJ, Lee SW, Oh JS, de Luis-Garcia R, Savadjiev P, Alvarado JL, Kubicki M. Localized abnormalities in the cingulum bundle in patients with schizophrenia: a diffusion tensor tractography study. *NeuroImage: Clin*. 2014; 5:93–99. [PubMed: 25003032]
64. Chiu CH, Lo YC, Tang HS, Liu IC, Chiang WY, Yeh FC, et al. White matter abnormalities of fronto-striato-thalamic circuitry in obsessive-compulsive disorder: a study using diffusion spectrum imaging tractography. *Psychiatry Res Neuroimaging*. 2011; 192(3):176–182. [PubMed: 21546223]
65. Mori S, Oishi K, Jiang H, Jiang L, Li X, Akhter K, Toga AW. Stereotaxic white matter atlas based on diffusion tensor imaging in an ICBM template. *Neuroimage*. 2008; 40(2):570–582. [PubMed: 18255316]
66. Jang SH, Yeo SS. Thalamocortical tract between anterior thalamic nuclei and cingulate gyrus in the human brain: diffusion tensor tractography study. *Brain Imaging Behav*. 2013; 7(2):236–241. [PubMed: 23371564]
67. Shah A, Jhavar SS, Goel A. Analysis of the anatomy of the Papez circuit and adjoining limbic system by fiber dissection techniques. *J Clin Neurosci*. 2012; 19(2):289–298. [PubMed: 22209397]
68. Papez JW. A proposed mechanism of emotion. *Arch Neurol Psychiatry*. 1937; 38(4):725.
69. Morgane PJ, Galler JR, Mokler DJ. A review of systems and networks of the limbic forebrain/limbic midbrain. *Prog Neurobiol*. 2005; 75(2):143–160. [PubMed: 15784304]
70. Bindokas VP, Jordan J, Lee CC, Miller RJ. Superoxide production in rat hippocampal neurons: selective imaging with hydroethidine. *J Neurosci*. 1996; 16(4):1324–1336. [PubMed: 8778284]
71. Urano S, Sato Y, Otonari T, Makabe S, Suzuki S, Ogata M, Endo T. Aging and oxidative stress in neurodegeneration. *Biofactors*. 1998; 7(1–2):103–112. [PubMed: 9523034]
72. Butt AM, Fern RF, Matute C. Neurotransmitter signaling in white matter. *Glia*. 2014; 62(11):1762–1779. [PubMed: 24753049]
73. Salter MG, Fern R. NMDA receptors are expressed in developing oligodendrocyte processes and mediate injury. *Nature*. 2005; 438(7071):1167–1171. [PubMed: 16372012]

74. Atlante A, Calissano P, Bobba A, Giannattasio S, Marra E, Passarella S. Glutamate neurotoxicity, oxidative stress and mitochondria. *FEBS Lett.* 2001; 497(1):1–5. [PubMed: 11376653]
75. Song SK, Sun SW, Ramsbottom MJ, Chang C, Russell J, Cross AH. Demyelination revealed through MRI as increased radial (but unchanged axial) diffusion of water. *Neuroimage.* 2002; 17(3):1429–1436. [PubMed: 12414282]
76. Nair G, Tanahashi Y, Low HP, Billings-Gagliardi S, Schwartz WJ, Duong TQ. Myelination and long diffusion times alter diffusion-tensor-imaging contrast in myelin-deficient shiverer mice. *Neuroimage.* 2005; 28(1):165–174. [PubMed: 16023870]
77. Klawiter EC, Schmidt RE, Trinkaus K, Liang HF, Budde MD, Naismith RT, Benzinger TL. Radial diffusivity predicts demyelination in ex vivo multiple sclerosis spinal cords. *Neuroimage.* 2011; 55(4):1454–1460. [PubMed: 21238597]
78. Madden DJ, Bennett IJ, Burzynska A, Potter GG, Chen NK, Song AW. Diffusion tensor imaging of cerebral white matter integrity in cognitive aging. *BBA-Mol Basis Dis.* 2012; 1822(3):386–400.
79. Tucker-Drob EM, Briley DA. Continuity of genetic and environmental influences on cognition across the life span: a meta-analysis of longitudinal twin and adoption studies. *Psychol Bull.* 2014; 140(4):949. [PubMed: 24611582]
80. Lindenberger U, Nagel IE, Chicherio C, Li SC, Heekeren HR, Bäckman L. Age-related decline in brain resources modulates genetic effects on cognitive functioning. *Front Neurosci.* 2008; 2(2): 234–244. [PubMed: 19225597]
81. Papenberg G, Lindenberger U, Bäckman L. Aging-related magnification of genetic effects on cognitive and brain integrity. *Trends Cogn Sci.* 2015; 19(9):506–514. [PubMed: 26187033]
82. Catheline G, Periot O, Amirault M, Braun M, Dartigues JF, Auriacombe S, Allard M. Distinctive alterations of the cingulum bundle during aging and Alzheimer's disease. *Neurobiol Aging.* 2010; 31(9):1582–1592. [PubMed: 18829135]
83. Choo IH, Lee DY, Oh JS, Lee JS, Lee DS, Song IC, Woo JI. Posterior cingulate cortex atrophy and regional cingulum disruption in mild cognitive impairment and Alzheimer's disease. *Neurobiol Aging.* 2010; 31(5):772–779. [PubMed: 18687503]
84. Fellgiebel A, Müller MJ, Wille P, Dellani PR, Scheurich A, Schmidt LG, Stoeter P. Color-coded diffusion-tensor-imaging of posterior cingulate fiber tracts in mild cognitive impairment. *Neurobiol Aging.* 2005; 26(8):1193–1198. [PubMed: 15917103]
85. Nir TM, Jahanshad N, Villalon-Reina JE, Toga AW, Jack CR, Weiner MW, et al. Effectiveness of regional DTI measures in distinguishing Alzheimer's disease, MCI, and normal aging. *NeuroImage: Clin.* 2013; 3:180–195. [PubMed: 24179862]
86. Santiago C, Herrmann N, Swardfager W, Saleem M, Oh PI, Black SE, Lanctôt KL. White matter microstructural integrity is associated with executive function and processing speed in older adults with coronary artery disease. *Am J Geriatr Psychiatry.* 2015; 23(7):754–763. [PubMed: 25499674]
87. Laukka EJ, Lövdén M, Kalpouzos G, Li TQ, Jonsson T, Wahlund LO, et al. Associations between white matter microstructure and cognitive performance in old and very old age. *PloS One.* 2013; 8(11):e81419. [PubMed: 24282593]
88. Yu Q, Peng Y, Mishra V, Ouyang A, Li H, Zhang H, et al. Microstructure, length, and connection of limbic tracts in normal human brain development. *Front Aging Neurosci.* 2014; 6:228. [PubMed: 25221509]
89. Huang TT, Leu D, Zou Y. Oxidative stress and redox regulation on hippocampal-dependent cognitive functions. *Arch Biochem Biophys.* 2015; 576:2–7. [PubMed: 25797440]
90. Buckner RL, Sepulcre J, Talukdar T, Krienen FM, Liu H, Hedden T, Johnson KA. Cortical hubs revealed by intrinsic functional connectivity: mapping, assessment of stability, and relation to Alzheimer's disease. *J Neurosci.* 2009; 29(6):1860–1873. [PubMed: 19211893]
91. Andrews-Hanna JR, Snyder AZ, Vincent JL, Lustig C, Head D, Raichle ME, Buckner RL. Disruption of large-scale brain systems in advanced aging. *Neuron.* 2007; 56(5):924–935. [PubMed: 18054866]
92. Damoiseaux JS, Beckmann CF, Arigita ES, Barkhof F, Scheltens P, Stam CJ, et al. Reduced resting-state brain activity in the default network in normal aging. *Cereb Cortex.* 2008; 18(8): 1856–1864. [PubMed: 18063564]

93. Hu J, Feng F, Zhu S, Sun L, Li G, Jiang N, Niu Y. Catalase C-262T polymorphism and risk of prostate cancer: evidence from meta-analysis. *Gene*. 2015; 558(2):265–270. [PubMed: 25576221]
94. Saadat M, Saadat S. Genetic polymorphism of CAT C-262T and susceptibility to breast cancer, a case-control study and meta-analysis of the literatures. *Pathol Oncol Res*. 2015; 21(2):433–437. [PubMed: 25248722]
95. Liu Y, Xie L, Zhao J, Huang X, Song L, Luo J, et al. Association between catalase gene polymorphisms and risk of chronic hepatitis B, hepatitis B virus-related liver cirrhosis and hepatocellular carcinoma in Guangxi population: a case-control study. *Medicine*. 2015; 94(13)
96. Plemenitas A, Kastelic M, Porcelli S, Serretti A, Makovec MR, Plesnicar BK, Dolžan V. Genetic variability in CYP2E1 and catalase gene among currently and formerly alcohol-dependent male subjects. *Alcohol Alcohol*. 2014:agu088.
97. Khodayari S, Salehi Z, Fakhrieh Asl S, Aminian K, Mirzaei Gisomi N, Torabi Dalivandan S. Catalase gene C-262T polymorphism: importance in ulcerative colitis. *J Gastroenterol Hepatol*. 2013; 28(5):819–822. [PubMed: 23425094]
98. Babusikova E, Jesenak M, Evinova A, Banovcin P, Dobrota D. Frequency of polymorphism-262C/T in catalase gene and oxidative damage in Slovak children with bronchial asthma. *Arch Bronconeumol*. 2013; 49(12):507–512. [PubMed: 23827365]
99. Taniguchi N, Konno S, Isada A, Hattori T, Kimura H, Shimizu K, et al. Association of the CAT-262C > T polymorphism with asthma in smokers and the nonemphysematous phenotype of chronic obstructive pulmonary disease. *Ann Allergy Asthma Immunol*. 2014; 113(1):31–36. [PubMed: 24824229]
100. Capurso C, Solfrizzi V, D'Introno A, Colacicco AM, Capurso SA, Bifaro L, et al. Short arm of chromosome 11 and sporadic Alzheimer's disease: catalase and cathepsin D gene polymorphisms. *Neurosci Lett*. 2008; 432(3):237–242. [PubMed: 18248894]
101. Petrovic D. Association of the — 262C/T polymorphism in the catalase gene promoter and the C242T polymorphism of the NADPH oxidase P22phox gene with essential arterial hypertension in patients with diabetes mellitus type 2. *Clin Exp Hypertens*. 2014; 36(1):36–39. [PubMed: 23701472]
102. Galecki P, Szemraj J, Zboralski K, Florkowski A, Lewinski A. Relation between functional polymorphism of catalase gene (-262C > T) and recurrent depressive disorder. *Neuro Endocrinol Lett*. 2009; 30(3):357–362. [PubMed: 19855359]
103. Forsberg L, Lyrenäs L, Morgenstern R, de Faire U. A common functional CT substitution polymorphism in the promoter region of the human catalase gene influences transcription factor binding, reporter gene transcription and is correlated to blood catalase levels. *Free Radical Biol Med*. 2001; 30(5):500–505. [PubMed: 11182520]
104. Wheeler-Kingshott CA, Cercignani M. About axial and radial diffusivities. *Magn Reson Med*. 2009; 61(5):1255–1260. [PubMed: 19253405]

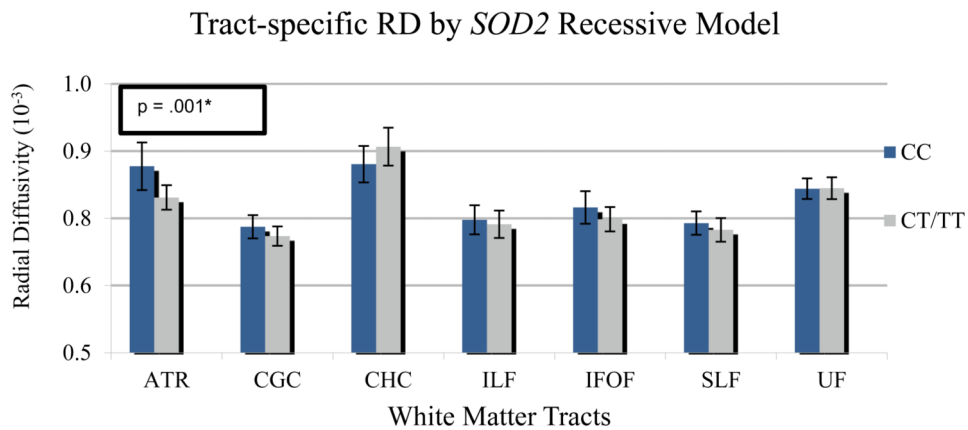


Fig. 1. Significant multivariate main effects were observed for tract-specific alterations in radial diffusivity (RD) when individuals were grouped according to the *SOD2* recessive model. Values were graphed according to raw RD values for visualization purposes. The p value .001 reflects significant group differences after the log₁₀ transformation, which survived the FDR correction. ATR = anterior thalamic radiation, CGC = cingulate gyrus segment of cingulum, CHC = hippocampal segment of cingulum, ILF = inferior longitudinal fasciculus, IFOF = inferior fronto-occipital fasciculus, UF = uncinate fasciculus.

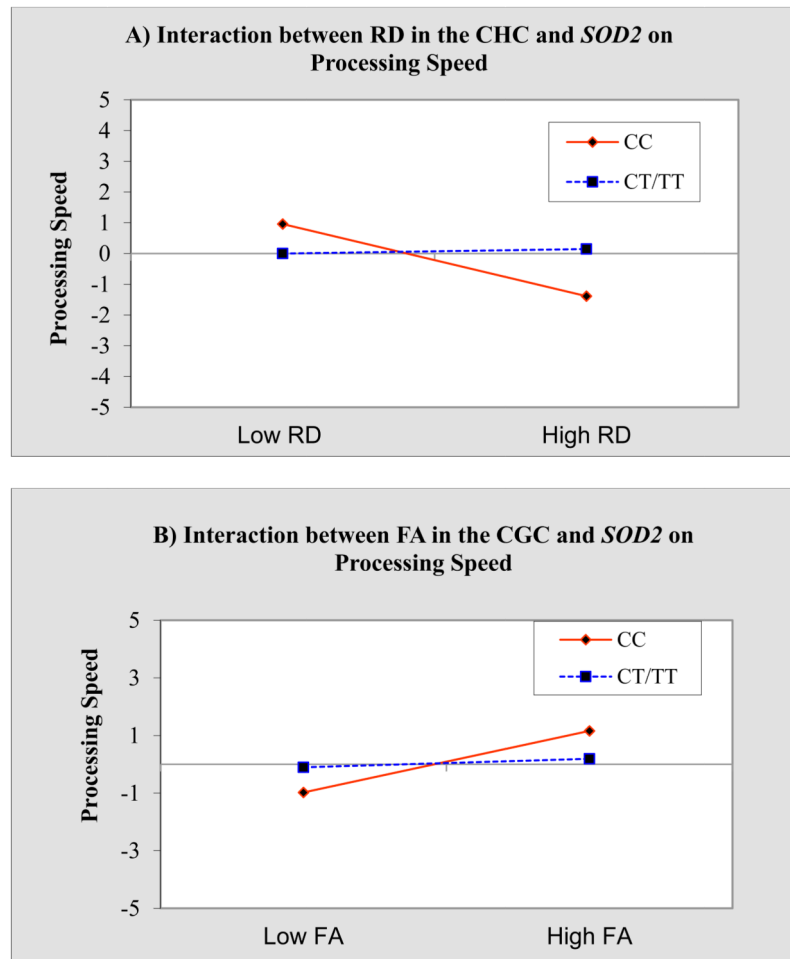


Fig. 2. Moderation of the *SOD2* CC genotype on radial diffusivity (RD) in the hippocampal segment of the cingulum (CHC) (A) and fractional anisotropy (FA) in the cingulate gyrus segment of the cingulum (CGC) (B) on processing speed. Endpoints were plotted according to mean centered maximum and minimum log transformed RD values (max = .27, min = -.06) and mean centered FA values (max = .09, min = -.01). Maximum and minimum FA values were normally distributed and not log transformed.

Table 1

Descriptive Characteristics of the Sample.

Total Sample (N = 94)			
Age (<i>M, SD</i>)	63.5 (8.2)		
Years of Education (<i>M, SD</i>)	15.6 (2.5)		
Sex (<i>n</i>) (Male, Female)	36, 60		
Race (% Caucasian)	75%		
Hypertension (<i>n</i> = Yes)	27		
<i>SOD2</i>	CC (<i>n</i> = 26)	CT/TT (<i>n</i> = 68)	<i>p</i> value
Age (<i>M, SD</i>)	64.50 (8.2)	63.16 (8.3)	0.481
Years of Education (<i>M, SD</i>)	14.88 (2.6)	15.86 (2.4)	0.053
Sex (<i>n</i>) (Male, Female)	9, 17	25, 43	0.846
Race (% Caucasian)	76.9	75.0	0.623
Hypertension (<i>n</i> = Yes)	8	19	0.571
<i>CAT-262</i> (% CC genotype)	57.7	66.2	0.444
<i>CAT</i>	CC (<i>n</i> = 60)	CT/TT (<i>n</i> = 34)	<i>p</i> value
Age (<i>M, SD</i>)	62.5 (8.3)	64.5 (7.3)	0.236
Years of Education	15.8 (2.4)	15.5 (2.5)	0.614
Sex (<i>n</i>) (Male, Female)	20, 40	14, 20	0.447
Race (% Caucasian)	68.3	88.2	0.052
Hypertension (<i>n</i> = Yes)	17	10	0.984
<i>SOD2</i> (% CC genotype)	48.4	52.4	0.777

Table 2

Significant and Trending Regression Models by Cognitive Domain.

A) Processing Speed									
	β	R ²	F	Sig	F	Model p	t	Variable p	f ²
ATR									
¹ AD	-.440	.172	13.5	-	<.001*		-3.85	<.001*	.21
² SOD2	-.109	.177	6.88	.557	.002		-.926	.358	.22
³ Interaction	.164	.202	5.32	.165	.002		1.41	.165	.25
¹ RD	-.362	.126	9.40	-	.003*		-2.95	.004*	.14
² SOD2	-.152	.138	5.14	.347	.009		-1.21	.230	.16
³ Interaction	.139	.155	3.86	.268	.013		1.12	.268	.18
CHC									
¹ AD	-.073	.002	.133	-	.717		-.585	.561	.00
² SOD2	.001	.002	.066	.979	.936		.011	.991	.00
³ Interaction	.261	.070	1.50	.041	.225		2.09	.041	.08
¹ RD	-.172	.025	1.60	-	.211		-1.44	.155	.03
² SOD2	-.012	.025	.786	.969	.460		-1.04	.918	.03
³ Interaction	.345	.144	3.37	.005*	.024*		2.89	.005*	.17
CGC									
¹ FA	.264	.057	3.92	-	.052		2.21	.031	.06
² SOD2	-.098	.059	2.01	.704	.143		-.803	.425	.06
³ Interaction	-.266	.127	3.06	.030*	.035*		-2.22	.030*	.15
¹ AD	-.341	.100	7.20	-	.009*		-2.65	.010*	.11
² SOD2	.023	.100	3.51	.832	.034		.190	.850	.11
³ Interaction	.067	.104	2.44	.604	.072		.522	.604	.12
¹ RD	-.443	.193	15.6	-	<.001*		-3.91	<.001*	.24
² SOD2	-.117	.201	8.07	.430	.001		-1.02	.311	.25
³ Interaction	.159	.226	6.12	.164	.001		1.41	.164	.29
IFOF									
¹ FA	.441	.211	17.1	-	<.001*		3.90	<.001*	.27

A) Processing Speed									
	β	R ²	F	Sig F	Model p	t	Variable p	f ²	
² SOD2	-.026	.212	8.46	.842	.001	-.235	.815	.27	
³ Interaction	-.129	.228	6.12	.256	.001	-1.15	.256	.30	
¹ AD	-.341	.102	7.31	-	.009*	-2.75	.008*	.11	
² SOD2	-.084	.110	3.89	.474	.026	-.655	.515	.12	
³ Interaction	-.017	.110	2.56	.893	.063	-.136	.893	.12	
¹ RD	-.465	.213	17.3	-	<.001*	-4.01	<.001*	.27	
² SOD2	-.098	.220	8.91	.430	<.001	-8.54	.396	.28	
³ Interaction	.064	.224	5.98	.582	.001	.553	.583	.29	
ILF									
¹ FA	.495	.243	20.8	-	<.001*	4.43	<.001*	.32	
² SOD2	-.013	.243	10.3	.904	<.001	-1.17	.907	.32	
³ Interaction	.013	.243	6.74	.905	.001	.119	.905	.32	
¹ RD	-.452	.194	15.6	-	<.001*	-4.02	<.001*	.23	
² SOD2	-.033	.194	7.71	.845	.001	-.294	.770	.23	
³ Interaction	.126	.210	5.58	.266	.002	1.12	.266	.27	
SLF									
¹ AD	-.389	.141	10.6	-	.002*	-3.08	.003*	.16	
² SOD2	-.053	.143	5.33	.679	.007	-.442	.660	.17	
³ Interaction	.023	.143	3.51	.855	.020	.183	.855	.17	
¹ RD	-.340	.110	7.99	-	.006*	-2.84	.006*	.20	
² SOD2	-.054	.112	4.02	.700	.023	-.452	.653	.13	
³ Interaction	.066	.116	2.75	.582	.050	.554	.582	.13	
UF									
¹ AD	-.411	.170	13.3	-	.001*	-3.49	.004*	.20	
² SOD2	-.021	.170	6.57	.848	.003	-.186	.817	.20	
³ Interaction	-.008	.170	4.32	.943	.008	-.071	.807	.20	
¹ RD	-.381	.142	10.8	-	.002*	-3.25	.002*	.16	
² SOD2	-.001	.142	5.32	.993	.007	-.009	.993	.16	
³ Interaction	.038	.144	3.53	.747	.020	.324	.747	.17	

A) Processing Speed						
	β	R ²	F	Sig F	Model p	Variable p
B) Executive Function						
	β	R ²	F	Sig F	Model p	Variable p
ATR						
¹ AD	-.311	.083	5.67	–	.020*	–2.52 .014*
² SOD2	–.137	.097	3.32	.325	.043	–1.08 .283
³ Interaction	.065	.101	2.28	.609	.089	.514 .609
CGC						
¹ RD	–.274	.061	4.10	–	.047*	–2.18 .033*
² SOD2	–.121	.077	2.57	.312	.085	–.952 .345
³ Interaction	–.036	.078	1.72	.777	.173	–.284 .777
IFOF						
¹ FA	.427	.171	12.8	–	.001*	3.61 .001*
² SOD2	–.090	.179	6.66	.432	.002	–.770 .444
³ Interaction	.065	.183	4.49	.585	.007	.549 .585
¹ RD	–.389	.124	8.80	–	.004*	–3.15 .003*
² SOD2	–.136	.144	5.14	.239	.009	–1.11 .271
³ Interaction	–.056	.147	3.45	.648	.022	–.459 .648
ILF						
¹ FA	.495	.243	20.8	–	<.001*	4.43 <.001*
² SOD2	–.013	.243	10.3	.904	<.001	–.117 .907
³ Interaction	.013	.243	6.74	.905	.001	.119 .905
¹ RD	–.258	.064	4.31	–	.042*	–2.56 .043*
² SOD2	–.074	.071	2.39	.485	.100	–.086 .491
³ Interaction	–.023	.071	1.57	.993	.207	–.001 .993
SLF						
¹ AD	–.268	.086	5.97	–	.017*	–2.04 .045*
² SOD2	–.089	.099	3.39	.364	.040	–.716 .477

A) Processing Speed								
	β	R ²	F	Sig F	Model <i>p</i>	t	Variable <i>p</i>	<i>f</i> ²
¹ Interaction	-.106	.108	2.46	.425	.071	-.803	.425	.12
UF								
¹ AD	-.276	.076	5.21	–	.026*	–2.20	.031*	.09
² <i>SOD2</i>	-.070	.084	2.84	.474	.066	–.706	.483	.09
³ Interaction	–0.14	.084	1.87	.923	.144	–.098	.923	.09
C) Memory								
	β	R ²	F	Sig F	Model <i>p</i>	t	Variable <i>p</i>	<i>f</i> ²
ATR								
ILF								
¹ FA	.262	.060	4.32	–	.041*	2.18	.034*	.06
² <i>SOD2</i>	.084	.066	2.38	.494	.100	.711	.480	.07
³ Interaction	.097	.075	1.79	.426	.157	.800	.426	.08

Note. Superscript numerals 1–3 denote the block in which each predictor variable was entered into the regression model. Statistical significance was determined by examination of the model *p* for main effects, and both the model *p* and significant change in *F* for interaction effects. FDR corrections were applied separately to main effects and interactions at the variable level. Values with an asterisk denote trend effects that did not survive FDR (trends are not noted for block 2 or 3 unless both the significant *F* change and model *p* are < .05). Bolded models with an asterisk survived the FDR corrected threshold at 63 comparisons. No interaction models survived the FDR threshold (*q* < .0007). ATR = anterior thalamic radiation, CGC = cingulate gyrus segment of cingulum, CHC = hippocampal segment of cingulum, ILF = inferior longitudinal fasciculus, IFOF = inferior fronto-occipital fasciculus, UF = uncinate fasciculus.